Horizontal Propagation Through Periodic Vegetation Canopies

Ahad Tavakoli, Kamal Sarabandi, and Fawwaz Ulaby

Radiation Laboratory
Department of Electrical Engineering and Computer Science
University of Michigan
Ann Arbor, MI 48109

ABSTRACT

A two-dimensional model has been developed to explain wave propagation through man-made vegetation canopies. The model is intended for media containing vertical cylinders, representing the stalks, and randomly oriented disks, representing the leaves. The model is a field approach, thereby accounting for all coherent, multiple interactions occuring in the canopy. The experimental component of this study includes measurements of the attenuation and phase shift patterns for horizontally and vertically polarized waves transmitted through a fully grown canopy of corn plants observed at 1.5 GHz. The model was found to provide excellent agreement with the experimental results.

1 INTRODUCTION

Location, spacing, and density of plants in most natural vegetation cover tend to be random in character. In some agricultural canopies, the location and density of plants are deterministic quantities, with some random fluctuations. Many man-made vegetation canopies are planted in a row arrangement. For such a vegetation cover, the random-medium techniques, as reported in the literature, are not applicable.

The present study is a deterministic field approach to the general problem of cylindrical wave propagation through a medium comprised of a one-dimensional periodic row structure with known row periodicity, known within-row stalk periodicity, and sporadic distribution of leaves. The vegetation canopy is divided into slabs (rows) that statistically exhibit the same electromagnetic properties. For a given incident direction, transmission through and reflection by an individual slab occurs at only a specific set of directions determined from Bragg-mode theory. After deriving the transmission and reflection coefficient matrices corresponding to the Bragg modes for a single slab, network theory is applied to derive the overall transmission and reflection coefficient matrices of the entire canopy. The overall transmitted field due to the cylindrical incident wave is then calculated by taking the inverse Fourier transform of the product of the total transmission coefficient spectrum of the medium and the angular spectrum of the incident field. Because the model is based on a coherent field approach, both the phase and amplitude of the propagating field can be calculated.

2 EXPERIMENTAL PROCEDURE

Using the configuration shown in Figure 1, the phase and magnitude of the wave transmitted through seven rows of a corn canopy were measured for both vertical and horizontal polarizations at 1.5 GHz. The receiver on the truck was stationary and the transmitter was made to glide along a rail system at the same height above the ground (1.2 m) as the receivers. Vertical and horizontal polarizations were transmitted simultaneously and the detected power and phase of the received fields were recorded using an HP-8510 network analyzer. Propagation measurements with and without leaves were performed to study the effects of individual crop constituents. At the end of the experiment, the corn plants were cut and removed and direct line-of-sight measurements were conducted for calibration purposes. The moisture contents, sizes, and densities of each constituent of the canopy were measured for incorporation in the theoretical calculations.

As an example of the collected data, Figure 3a,b shows a comparison of the measured magnitudes and phases for a vertically polarized wave with and without the canopy (stalks and leaves) present. The data shows that the presence of the vegetation in the transmission path causes amplitude fluctuations and widens the beam of the power pattern. The data suggests that for H polarization, leaves are the dominant contributors to the loss suffered by the wave, but for V polarization, the stalks are the major attenuators of the electromagnetic wave.

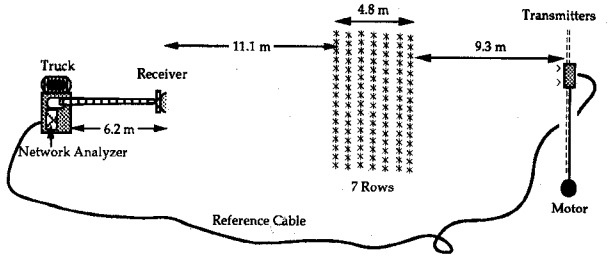

Figure 1. Measurement configuration showing the transmitter and receiver sections, both at the same height at 1.2 m above ground level. The transmitter platform was made to glide on a rail under motor control.

3 PROPAGATION MODEL FOR THE DEFOLIATED CANOPY

The following treatment pertains to a row-crop vegetation canopy comprised of vertically oriented stalks. A wave-structure propagation model (WSPM) is developed that relates the transmission and reflection proprerties of the medium to the transmitted wave pattern of a non-uniform incident wave.

3.1 A SINGLE SLAB OF PERIODICALLY DISTRIBUTED SCATTERERS

Consider a plane wave illuminating an array of periodically dis-

tributed scatterer at an incidence angle ϕ_0 (Fig. 2). The scattering from such a periodic structure can be formulated *via* an integral equation involving polarization currents whose domain is confined over a period L of the structure using Floquet's theorem [1]. The solutions of the integral equations can be obtained by numerical techniques, from which the scattered fields can then be calculated. The propagating scattered plane waves of this periodic structure are known as Bragg modes. For a plane wave incident at angle ϕ_0, the traveling direction of the m^{th} Bragg mode is defined by the angle γ_m (Fig. 2) such that:

$$\cos\gamma_m = \frac{m\lambda_0}{L} - \sin\phi_0 \tag{1}$$

where L is the spacing between scatterers and λ_0 is the wavelength. The m^{th} Bragg mode is a propagating one if

$$(-1+\sin\phi_0)\frac{L}{\lambda_0} \le m \le (1+\sin\phi_0)\frac{L}{\lambda_0} \tag{2}$$

If the separation between the cylinders is large enough so that the internal field of each cylinder is not affected by the fields of the other cylinders, the approximate solution derived by Sarabandi et al. [2] may be used instead. The scattering amplitude of the m^{th} Bragg mode is thus given by:

$$F_p^m = \frac{2}{Lk_a\sin\gamma_m}\left\{A_0^p + 2\sum_{\beta=1}^{\infty}\cos\left[\beta\left(\phi_0 \pm \gamma_m + \frac{\pi}{2}\right)\right]A_\beta^p\right\} \tag{3}$$

where k_a is the wave number of the homogeneous material surrounding the cylinders, and p denotes the wave polarization. The coefficients A_β^p are defined as:

$$A_\beta^V = \frac{n_c J_\beta(x_r)H_\beta^{(1)'}(y_r) - n_a J_\beta'(x_r)H_\beta^{(1)}(y_r)}{n_a J_\beta(y_r)H_\beta^{(1)'}(x_r) - n_c J_\beta'(y_r)H_\beta^{(1)}(x_r)} \tag{4}$$

for V polarization and

$$A_\beta^H = \frac{n_a J_\beta(x_r)H_\beta^{(1)'}(y_r) - n_c J_\beta'(x_r)H_\beta^{(1)}(y_r)}{n_c J_\beta(y_r)H_\beta^{(1)'}(x_r) - n_a J_\beta'(y_r)H_\beta^{(1)}(x_r)} \tag{5}$$

for H polarization, where n_c and n_a are the indices of refraction of the homogeneous cylinders and the surrounding homogeneous material, J_β and $H_\beta^{(1)}$ are the Bessel and Hankel functions of the first kind of order β, and the prime denotes derivative with respect to the argument. If k_a and k_c are the wave numbers of the surrounding homogeneous material and of the cylinders, respectively, and r is the radius of the cylinder, then $x_r = k_c r$ and $y_r = k_a r$.

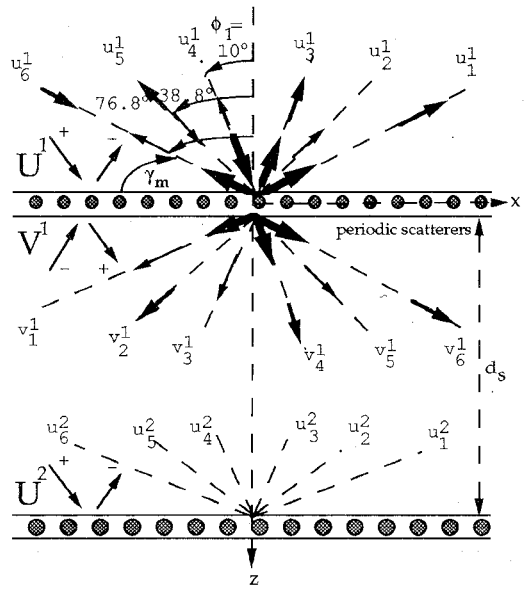

Figure 2. An example of a multi-port network for Bragg modes of an array of periodically distributed cylinders next to a slab of air.

3.2 TRANSMISSION AND REFLECTION COEFFICIENTS OF CASCADED SLABS

A slab of periodically distributed scatterers is conservative in terms of the number and directions of its Bragg modes. In other words, if the wave incident upon a slab from one of the Bragg-mode directions associated with the waves transmitted by the previous slab, the number of new Bragg modes will remain the same as for the previous slab. Therefore in a cascaded arrangement of identical slabs, the directions of multiple bounces between the slabs are quantized and limited to the directions associated with a single slab. Each Bragg mode direction can be considered a port of a multi-port system and network theory can be utilized to characterize the behavior of cascaded slabs. Figure 2 illustrates an example of such a slab when L, the period of the scatterers, is 1.25 λ. With superscripts denoting the slab number and subscripts denoting the port number, the plane waves incident from ports U_4^1, U_5^1, or U_6^1 will be scattered only into the 12 prescribed directions shown in Figure 2. Due to the symmetry of Bragg modes, incident waves from any of the other Bragg-mode directions will be scattered into the same directions constituted by ports 4, 5, and 6. Therefore, a 12-port network can completely represent the scattering behavior of the example shown in Figure 2. The reflection coefficient matrix, $[R_s]$, is defined such that R_{ij} represent the scattering amplitude of the plane wave scattered into port i due to a plane wave incident at port j on the same side of the slab. The transmission coefficient matrix, $[T_s]$, is defined similarly for the wave scattered into the other side of the slab.

With reference to Figure 2, the $\left[U^1\right]$ fields of the first slab are related to the $\left[U^2\right]$ fields of the second slab by a scattering matrix $[S]$,

$$\begin{bmatrix} U^{1+} \\ U^{1-} \end{bmatrix} = [S]\begin{bmatrix} U^{2+} \\ U^{2-} \end{bmatrix} \quad , \tag{6}$$

whose elements are given by

$$[S] = \begin{bmatrix} [T_s]^{-1}[\phi_1] & -[T_s]^{-1}[R_s][\phi_2] \\ [R_s][T_s]^{-1}[\phi_1] & [T_s][\phi_2] - [R_s][T_s]^{-1}[R_s][\phi_2] \end{bmatrix} \tag{7}$$

$[\phi_1]$ is a diagonal matrix with diagonal elements $e^{-ik_0 d_s\cos\phi_m}$, where m represents the port number and $[\phi_2]$ is the complex conjugate of $[\phi_1]$. For a periodic array of n slabs, the total ABCD matrix $[S_n]$ of the cascaded structure is:

$$[S_n] = [S]^n = \begin{bmatrix} [S_{n11}] & [S_{n12}] \\ [S_{n21}] & [S_{n22}] \end{bmatrix} \tag{8}$$

for a plane wave incident on the j^{th} port of the first slab, the total transmission and reflection coefficients of the resultant medium at ports i can be obtained from

$$T_{t_{ij}} = \left\{ \left[S_{n_{11}} \right]^{-1} \right\}_{ij} \tag{9}$$

and

$$R_{t_{ij}} = \left\{ \left[S_{n_{21}} \right] \left[S_{n_{11}} \right]^{-1} \right\}_{ij} \tag{10}$$

All multiple coherent wave scattering between the stalks has been taken into account in the above derivation.

3.3 PROPAGATION OF A NON-UNIFORM WAVE THROUGH CASCADED SLABS

The wave pattern incident on the canopy can be represented by the two-dimensional antenna angular spectrum:

$$\mathbf{U}^{inc} = \frac{1}{2\pi} \int_{-\infty}^{+\infty} \mathbf{A}(k_x) e^{ik_z z + ik_x x} dk_x \tag{11}$$

where $\mathbf{A}(k_x)$ is a complex function representing the Fourier transform of the field distribution on the transmitting antenna aperture. $\mathbf{A}(k_x)$ is in the y- direction and represents the electric field for a vertically polarized wave and the magnetic field for a horizontally polarized wave. The above representation of $\mathbf{U}^{inc}$ shows that the incident wave is the sum of an infinite number of plane waves travelling in the $(k_z\hat{\mathbf{z}} + k_x\hat{\mathbf{x}})$ direction, each having an amplitude $\frac{\mathbf{A}(k_x)}{2\pi}$. The field transmitted through the cascaded slabs is the product of the incident wave and the total transmission coefficient of the medium. Therefore, the transmitted wave will be the superposition of all transmitted plane waves with amplitudes $\frac{\mathbf{A}(k_x)\mathbf{T}_t(k_x)}{2\pi}$, where $\mathbf{T}_t(k_x)$ is the total transmission coefficient of the cascaded slabs for incident angle $\phi_0 = \tan^{-1}\left(\frac{k_x}{k_z}\right)$.

At the transmit antenna, the incident field is equal to the Fourier transform of $\mathbf{A}(k_x)$. If we shift the reference from the antenna aperture to the edge of the canopy at a distance z_{tc} away, then the incident field at that point becomes equal to the Fourier transform of the function

$$\mathbf{F}(k_x) \equiv \mathbf{A}(k_x) e^{ik_z z_{tc}} \ . \tag{12}$$

The total transmitted wave can now be obtained by taking the inverse Fourier transform of the product of $\mathbf{F}(k_x)$ and the total transmission coefficient of the medium, $\mathbf{T}_t(k_x)$. Thus

$$\mathbf{U}^{tr} = \frac{1}{2\pi} \int_{-\infty}^{+\infty} \mathbf{F}(k_x) \mathbf{T}_t(k_x) e^{ik_x x} dk_x \tag{13}$$

The reflected wave pattern can be derived in a similar fashion. The function $\mathbf{F}(k_x)$ may be represented by:

$$\mathbf{F}(k_x) = \int_{-\infty}^{+\infty} \mathbf{f}(x) e^{-ik_x x} dx \tag{14}$$

where $\mathbf{f}(x)$ is the incident wave pattern at the edge of the canopy. Assuming a one dimensional uniform field distribution at the aperture of the transmitting antenna, $\mathbf{f}(x)$ can be asymptotically approximated by:

$$\mathbf{f}(x) = \frac{1}{\sqrt{\rho}} e^{ik_0\rho\cos\phi} \frac{\sin(\alpha k_0 \sin\phi)}{\alpha k_0 \sin\phi} \hat{\mathbf{y}} \tag{15}$$

where α is a function of the antenna size, frequency, and polarization, ϕ is the angle measured from the boresight direction of the transmitting antenna, and ρ is the distance the wave travels at the angle ϕ from transmitter to the edge of the canopy. Using the measured reference data, α can be estimated such that the simulated reference pattern is the same as that of the reference field.

4 COMPARISON WITH EXPERIMENTAL DATA

The model introduced in the preceding section was applied to configurations for which experimental data are available. Figure 3 compares the resultant amplitude and phase of a simulated canopy of seven rows of stalks with measured data at 1.5 GHz for vertical polarization. Parts (a) and (b) are the measured amplitude and phase patterns and parts (c) and (d) are the calculated results. The canopy parameters are given in the figure caption.

The simulation results are in good agreement with the experimental measurements for the overall pattern, attenuation level, and the peak to peak variation of power exhibited by the measurements. The simulated phase complies with the measured data in predicting that the field in the canopy leads the reference field. Figure 4 displays the same calculation for horizontal polarization. Both the pattern and the attenuation level of the simulation are in excellent agreement with the measured data. The phase calculation reconfirms that the canopy phase at horizontal polarization, unlike the vertical polarization, lags the reference phase. It should also be noted that the simulation underestimates the attenuation level by about 2 dB for horizontal polarization. This is attributed to the fact that the stalks in the canopy are not perfectly vertical and the component of the field parallel to the cylinders is attenuated by an amount proportional to the attenuation for vertical polarization.

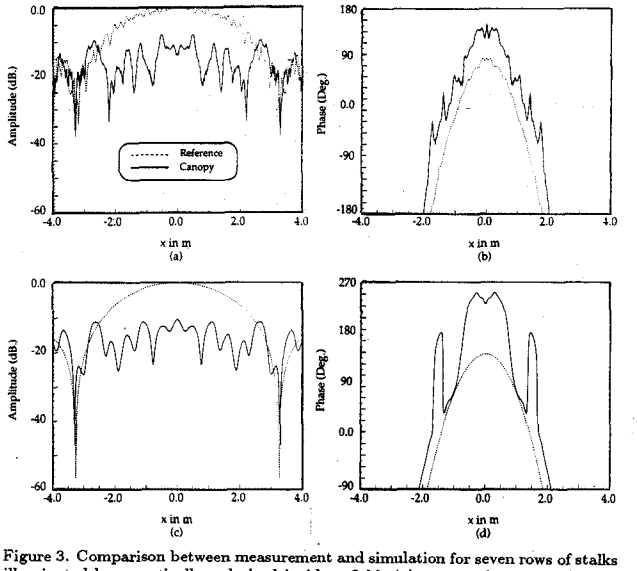

Figure 3. Comparison between measurement and simulation for seven rows of stalks illuminated by a vertically polarized incident field; (a) measured power, (b) measured phase, (c) simulated power, and (d) simulated phase. The canopy parameters are d_s = 77.3 cm, L = 25 cm, diameter of the stalks = $2r$ = 1.75 cm, and $\epsilon_s = 36 + i10$.

5 PROPAGATION MODEL FOR A FULL CANOPY

At wavelengths much longer than the dimensions of a leaf, the leaves in a canopy exhibit weak scattering properties, and their presence serves primarily to alter the effective dielectric constant of the background medium surrounding the stalks. If we treat the leaves as randomly oriented disks with volume fraction v_ℓ, the equivalent dielectric constant of the medium is given then by the mixing model [3]:

$$\epsilon_a = 1 + v_\ell(\epsilon_\ell - 1)\left(2 + \frac{1}{\epsilon_\ell}\right) \tag{16}$$

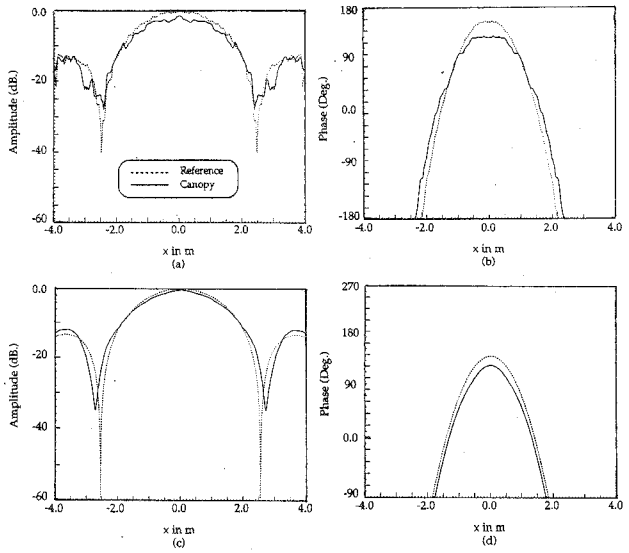

Figure 4. Comparison between measurement and simulation for seven rows of stalks illuminated by a horizontally polarized incident fie ld; (a) measured power, (b) measured phase, (c) simulated power, (d) simulated phase. The canopy parameters are the same as in Figure 6.

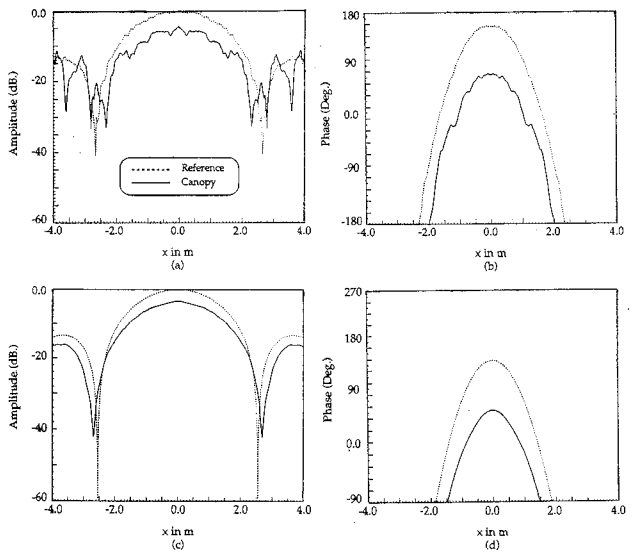

Figure 6. Comparison between measurement and simulation for seven rows of a full canopy of both stalks and leaves illuminated by a horizontally polarized incident field; (a) measured power, (b) measured phase, (c) simulated power, and (d) simulated phase. The canopy parameters are the same as for Figure 8.

where ϵ_ℓ is the dielectric constant of the leaf material, for which expressions relating it to the leaf moisture content are available in the literature [4]. This model was applied to the seven rows of stalks with leaves at 1.5 GHz. Figures 5 and 6 compare model results with measured data for vertical and horizontal polarizations, respectively. The pattern, oscillation, and attenuation levels are in very good agreement with the measured data. It should be noted that for vertical polarization, the field transmitted through the stalk canopy leads the reference field, but the opposite is true for the leaf canopy. Therefore, these two phenomena tend to cancel each other's effects when both stalks and leaves are present, which is supported by both the simulation and the measured data.

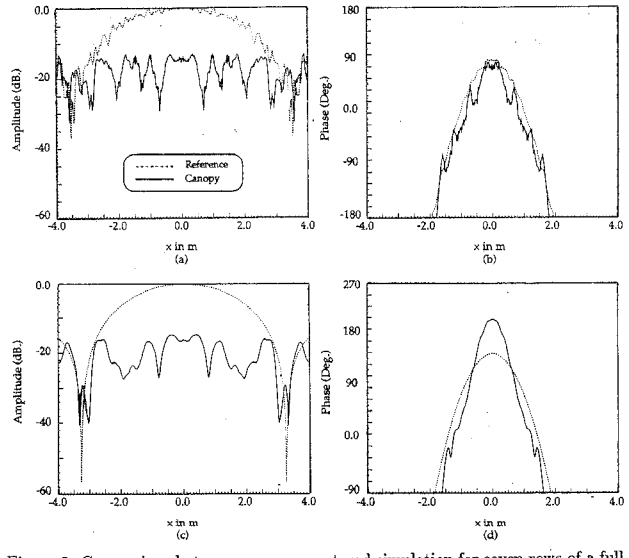

Figure 5. Comparison between measurement and simulation for seven rows of a full canopy of both stalks and leaves illuminated by a vertically polarized incident field; (a) measured power, (b) measured phase, (c) simulated power, and (d) simulated phase. The canopy parameters are $d_s = 77.3$ cm, $L = 25$ cm, diameter of the stalks$= 2r = 1.75$ cm, $\epsilon_s = 36 + i10$, $\nu_1 = 7.5 \times 10^{-4}$, and $\epsilon_1 = 28 + i8$.

6 CONCLUSION

The propagation model developed in this paper is a deterministic field approach to the solution of wave propagation through a man-made vegetation canopy comprised of stalks and leaves. Both multiple, coherent, wave scattering by the stalks and intrinsic absorption by the leaves are accounted for in the derivation. Excellent agreement between theory and experiment is obtained for canopies with and without leaves at 1.5 GHz.

References

[1] K. Sarabandi, "Study of Periodic Dielectric Surfaces: Simulation with Anisotropic Layers and Application to High Frequency Scattering from Corrugated Convex Bodies," Radiation Laboratory Report 02455-2-T, University of Michigan, February, 1990.

[2] K. Sarabandi, A. Tavakoli, and F.T. Ulaby, "Scattering from a Periodic Array of Dielectric Cylinders; An Approximate Solution," Radiation Laboratory Report 022557-4-T, University of Michigan, October, 1990.

[3] Ulaby, F.T., R.K. Moore, and A.K. Fung, *Microwave Remote Sensing: Active and Passive*, vol. 3, Artech House, 1986, Appendix E.

[4] M.A. El-Rayes, and F.T. Ulaby, "Microwave dielectric spectrum of vegetatio-part I: experimental observations," *IEEE Trans. Geosci. Remote Sensing*, vol. GE-25, no. 5, pp. 541-549, September, 1987.